Optical spectroscopy and band gap analysis of hybrid improper ferroelectric $Ca_3Ti_2O_7$

Judy G. Cherian,[1] Turan Birol,[2] Nathan C. Harms,[1] Bin Gao,[2,3] Sang-Wook Cheong,[2,3] David Vanderbilt,[2] and Janice L. Musfeldt[1,4,a)]
[1]*Department of Chemistry, University of Tennessee, Knoxville, Tennessee 37996, USA*
[2]*Department of Physics and Astronomy, Rutgers, The State University of New Jersey, Piscataway, New Jersey 08854, USA*
[3]*Rutgers Center for Emergent Materials, Rutgers, The State University of New Jersey, Piscataway, New Jersey 08854, USA*
[4]*Department of Physics, University of Tennessee, Knoxville, Tennessee 37996, USA*

(Received 5 March 2016; accepted 9 June 2016; published online 27 June 2016)

We bring together optical absorption spectroscopy, photoconductivity, and first principles calculations to reveal the electronic structure of the room temperature ferroelectric $Ca_3Ti_2O_7$. The 3.94 eV direct gap in $Ca_3Ti_2O_7$ is charge transfer in nature and noticeably higher than that in $CaTiO_3$ (3.4 eV), a finding that we attribute to dimensional confinement in the $n = 2$ member of the Ruddlesden-Popper series. While Sr substitution introduces disorder and broadens the gap edge slightly, oxygen deficiency reduces the gap to 3.7 eV and gives rise to a broad tail that persists to much lower energies. *Published by AIP Publishing*. [http://dx.doi.org/10.1063/1.4954404]

Ferroelectricity is one of the most useful and widely examined properties of the ABO_3 perovskites. $BaTiO_3$ and $PbTiO_3$ are flagship examples due to their spontaneous and switchable electric polarization.[1,2] The discovery of polarization in perovskite superlattices due to coupling of two rotational modes[3] motivated theoretical investigation that extended this idea to naturally occurring bulk materials that belong to the layered perovskite Ruddlesden-Popper ($A_{n+1}B_nX_{3n+1}$) series.[4,5] These studies identified two candidates as potential hybrid improper ferroelectrics: $Ca_3Ti_2O_7$ and $Ca_3Mn_2O_7$.[4,5] They are dubbed "improper" because ferroelectric polarization is not the primary order parameter, and the phrase "hybrid improper" indicates that the simultaneous onset of more than one primary order parameter (which are, in this case, octahedral rotations) is responsible for the emergence of the ferroelectric polarization.[6] While $Ca_3Ti_2O_7$ was already known to exist in a polar space group prior to these predictions,[4,7] the recent experimental discovery that it is indeed a switchable room temperature ferroelectric[8] is widely regarded as a materials design coup. This system sports a coercive field of 120 kV/cm and a net remanent electric polarization of 8 μC/cm^2—values that compare well with proper ferroelectrics.[8] For instance, $BaTiO_3$ and $BiFeO_3$ films have coercive fields of 200 kV/cm and 140 kV/cm, respectively.[9,10] Interestingly, $CaTiO_3$ does not have a ferroelectric phase because the transition is suppressed by octahedral rotations.[11–13] There are, however, ferroelectric domain walls.[14,15]

Unlike its close cousins (the prototypical titanate ferroelectric $BaTiO_3$ or strained Ruddlesden-Popper member $Sr_{n+1}Ti_nO_{3n+1}$ in which the polarization is driven by the displacement of the Ti cation),[17,18] the ferroelectric distortion in $Ca_3Ti_2O_7$ mostly involves displacement of the A-site Ca cations (Fig. 1).[8,19] The combined oxygen octahedral rotation/tilting modes that constitute the distortion result in layered dipoles that only partially cancel, yielding a net polarization due to the non-cancelling electric dipoles.[8] Charged domain walls (both ferroelectric and ferroelastic) are also present in this material.[8] The other physical properties are, at this time, unexplored. Clearly, the opportunity to investigate a recently discovered hybrid improper ferroelectric is a very exciting prospect. At the same time, the combination of octahedral rotations and ferroelectricity in this perovskite is unusual[13] and merits additional investigation.

In this Letter, we report the optical properties of ferroelectric $Ca_3Ti_2O_7$ and compare our findings with complementary first principles calculations. We find a direct band gap of 3.94 eV, noticeably larger than that of $CaTiO_3$ (3.4 eV). This

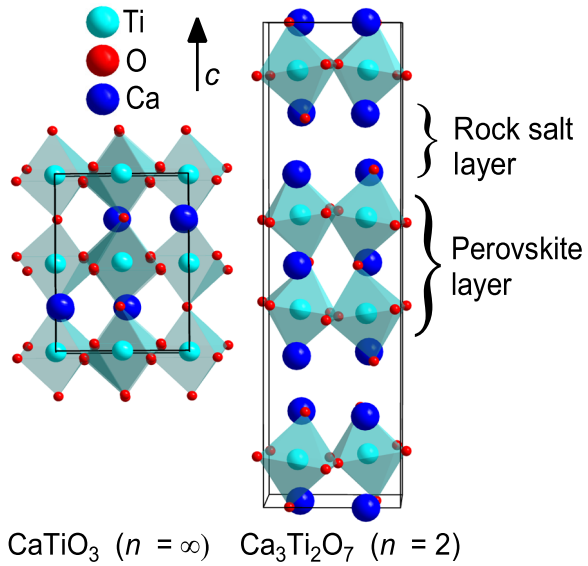

FIG. 1. (a) Crystal structure of $CaTiO_3$ illustrating the well-known three dimensionally connected octahedra of the $n = \infty$ material[16] and (b) the structure of $Ca_3Ti_2O_7$ which sports double layer slabs of perovskite units separated by CaO layers ($n = 2$).[7] The properties of the $A_{n+1}B_nX_{3n+1}$ homologous series are determined by the number of charge storage layers.

a)Electronic mail: musfeldt@utk.edu

is due to confinement effects in the $n=2$ member of the Ruddlesden-Popper series. Photoconductivity in $Ca_3Ti_2O_7$ tracks the absorption, with the largest response occurring just above the gap. We also explore the effects of *A*-site substitution and oxygen deficiency. Sr-substitution introduces disorder (which broadens the band edge slightly), whereas oxygen deficiency reduces the gap to 3.7 eV and gives rise to a broad tail that persists to much lower energies. These characteristics, combined with a natural ability to separate charge, suggest that $Ca_3Ti_2O_7$ and its derivatives may find applications in ultraviolet light harvesting and photo-catalysis.[20–22]

High-quality single crystals of $Ca_3Ti_2O_7$, $Ca_{2.5}Sr_{0.5}Ti_2O_7$, and $Ca_3Ti_2O_{7-\delta}$ were grown using the optical floating zone method as described in Ref. 8. The nominal value of δ is on the order of 0.001. We employed a series of spectrometers and a combination of transmittance and reflectance techniques (on thinner and thicker samples, respectively) to extract the absorption coefficients. Photoconductivity experiments were carried out on crystals with sputtered Pt contacts using a setup that includes a Xenon source, a source measurement unit, a series of narrow bandpass filters, and tungsten contact tips. The response was normalized for power intensity and area. All experiments were carried out at room temperature. First-principles calculations at the level of density functional theory (DFT) and generalized gradient approximation (GGA) were performed using the PBEsol exchange-correlation functional[23] and the projector augmented wave method[24,25] as implemented in VASP.[26–28] For the theoretical band gap, we report the energy difference between the highest occupied and lowest unoccupied Kohn-Sham states, which serves as a guide to understand band gap trends but does not directly correspond to a physically measurable quantity.

Figure 2 displays the optical properties of $Ca_3Ti_2O_7$ at room temperature. The absorption is low and flat until nearly 4 eV, beyond which there is a sharp increase that defines the band gap and higher energy series of electronic excitations. Comparison with other perovskites like $CaTiO_3$ suggests that these features should be assigned as O $2p \rightarrow$ Ti $3d$ charge transfer excitations.[29,30] Traditionally, the magnitude and nature of the allowed gap is determined from the spectroscopic response as

$$\alpha(E) = \frac{A}{E}(E - E_{g,dir})^{0.5} + \frac{B}{E}(E - E_{g,ind} \mp E_{ph})^2, \quad (1)$$

where $\alpha(E)$ is the absorption coefficient, $E_{g,dir}$ is the direct gap energy, $E_{g,ind}$ is the indirect gap energy, E_{ph} is the mediating phonon energy, and A and B are constants. Therefore, plots of $(\alpha E)^2$ vs energy and $(\alpha E)^{1/2}$ vs energy can reveal direct or indirect character via linear extrapolation to the energy axis.[31,32] As discussed in detail below, we find that $Ca_3Ti_2O_7$ has a direct gap of 3.94 eV. There is no evidence for indirect character. It is worth noting that, even though this type of analysis was developed for single parabolic band materials like traditional semiconductors,[32,33] it has been extended to include more complicated materials with non-parabolic bands such as oxides.[34–37]

In Figures 3(a) and 3(b), we display the band structure and the densities of states (DOS) of $Ca_3Ti_2O_7$ determined

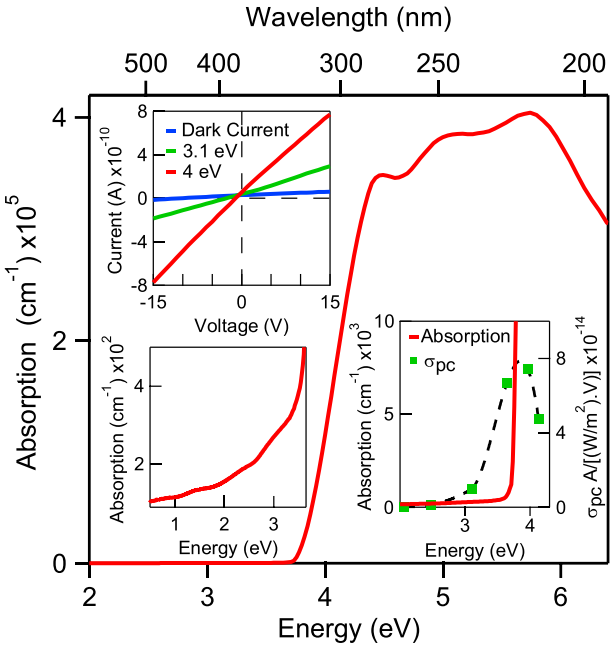

FIG. 2. Optical absorption spectrum of $Ca_3Ti_2O_7$ at 300 K. The 3.94 eV band gap derives from charge transfer excitations. The lower left-hand inset shows a close-up view of the data below 3.5 eV. The upper inset displays typical *I* - *V* curves taken in the dark and under 3.1 and 4 eV illumination. The lower right-hand inset compares the photoconductance taken at various photon energies along with the absorption coefficient. The black dashed curve is a guide to the eye.

from DFT. The Ti *d*-bands in $Ca_3Ti_2O_7$ are almost completely unoccupied and form the bottom of the conduction band, whereas the fully occupied oxygen *p* bands form the top of the valence band. This is also the case in $CaTiO_3$.[28] In both compounds, there is considerable hybridization between the

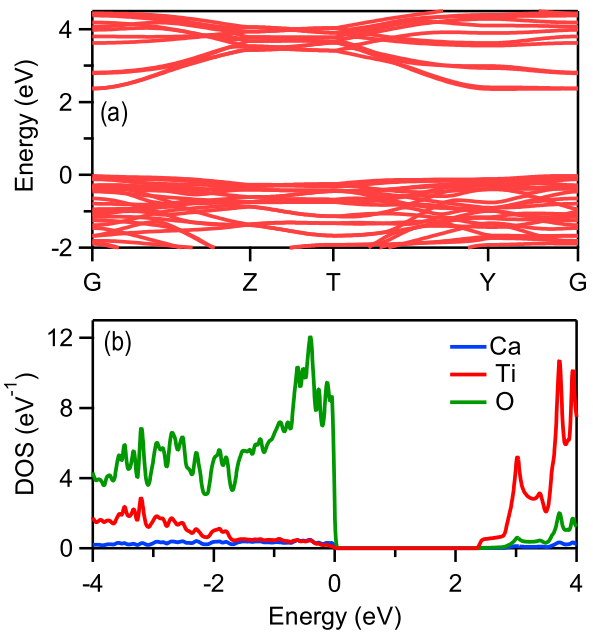

FIG. 3. (a) Band structure of $Ca_3Ti_2O_7$ (see the supplementary material for the definition of the high symmetry points in the Brillouin zone[28,38]). The bottom of the conduction band consists of dispersionless bands along the Γ-*Y* line (which is parallel to the crystallographic *c* axis), in line with the orbital projected DOS (shown in the supplementary material) that indicates that these bands consist of *d*-orbitals with lobes perpendicular to the *c* axis. (b) Densities of states per formula unit and projected onto the different atomic species.

oxygen and titanium states, with a negligible amount of Ca density of states around the Fermi level. Even though the parent perovskite and Ruddlesden-Popper structures result in different symmetry environments for the ions, we find that the basic features of the band structure are similar, which is not surprising, given their band insulating behaviours.

We note that, according to our calculations, the band gap of $Ca_3Ti_2O_7$ (2.38 eV) is slightly larger than that of $CaTiO_3$ (2.30 eV). While DFT at the level of local density approximation (LDA) (or GGA) is usually considered sufficient to capture the trends of gaps in band insulators with different crystal structures, it was reported in Ref. 39 that the trend of the gap between the bulk perovskite $SrTiO_3$ and the Ruddlesden-Popper compounds $Sr_{n+1}Ti_nO_{3n+1}$ is not correctly reproduced by DFT. However, DFT correctly captures the trends of the band gaps between different members of the $Sr_{n+1}Ti_nO_{3n+1}$ Ruddlesden-Popper series. Since the Ti *d*-states are unoccupied, this is probably not an error associated with the absence of strong on-site correlation effects in DFT. Rather, it might be necessary to calculate the full optical response, including the effect of electron-hole interactions, to capture the correct trend of the band gaps,[39] which is beyond the scope of this work. At this stage, we merely note that if the $CaTiO_3$ related compounds behave similarly to their closely related $SrTiO_3$ cousins, we would anticipate $Ca_3Ti_2O_7$ to have an even larger gap than $CaTiO_3$ in the light of our calculations and previous work on $Sr_{n+1}Ti_nO_{3n+1}$.[39] This point is verified by our measurements as discussed below.

We also sought to evaluate the ability of $Ca_3Ti_2O_7$ to create photocarriers. The upper inset of Fig. 2 displays typical *I-V* curves with light on and off, and the lower right-hand inset shows the photoconductance at different illumination energies. Clearly, there is a strong correlation between the absorption coefficient and photoconductivity. Moreover, it is well known that photocurrent increases near or above the band gap.[41] This is because photoconductivity is related to absorption as[42] $\sigma_{PC} \propto \eta\alpha(E)\tau$, where σ_{PC} is the photoconductance of the sample, η is the quantum efficiency (defined as ratio of excited carriers created to the number of incident photons), $\alpha(E)$ is the absorption, and τ is the carrier life time. From this expression, it is clear that as absorption rises, the photoconductance should also increase. This trend is evident in the similarity between σ_{PC} and $\alpha(E)$. Our analysis shows that current loss takes place predominantly via space-charge-limited conduction, similar to the mechanism in other perovskites.[43,44] We estimate a charge mobility on the order 10^{-4} $cm^2/V{\cdot}s$.

Figure 4 summarizes the optical absorption and direct gap analysis of $Ca_3Ti_2O_7$ and compares the findings with those of $CaTiO_3$, $Ca_{2.5}Sr_{0.5}Ti_2O_7$, and $Ca_3Ti_2O_{7-\delta}$. This series provides a platform with which we can assess the structure-property relationships connected with dimensionality and confinement, *A*-site substitution-related disorder, and oxygen deficiency.

Comparing the optical response and band gap analysis of $Ca_3Ti_2O_7$ and $CaTiO_3$,[40] we immediately notice that the onset of charge transfer excitations in $Ca_3Ti_2O_7$ occurs at a higher energy than that in the $n = \infty$ member of the Ruddlesden-Popper series. As reported previously, the direct gap of $CaTiO_3$ is 3.4 eV.[40] This comparison (3.94 vs. 3.4 eV) immediately reveals the effect of reduced dimensionality on the electronic properties. A similar variation has been

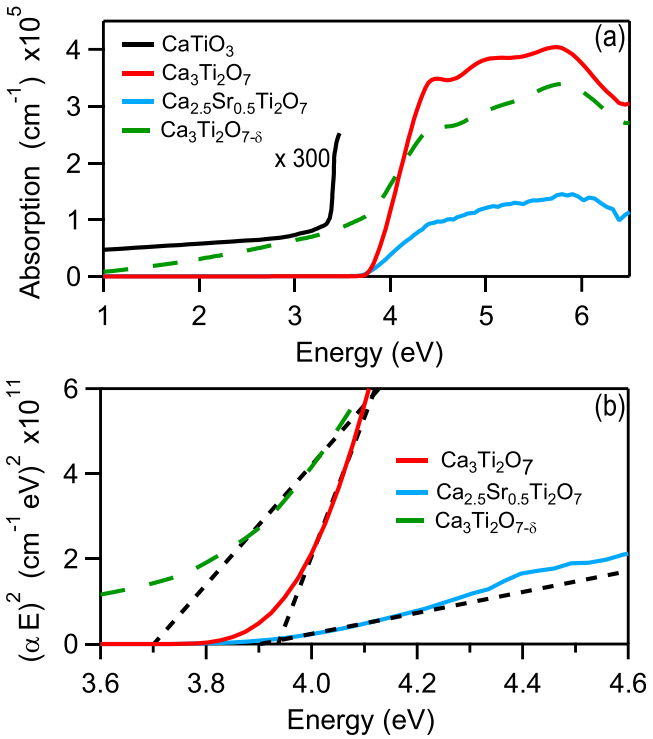

FIG. 4. (a) Absorption spectrum of $Ca_3Ti_2O_7$ along with that of the Sr-substituted counterpart and the oxygen deficient analog. The response of $CaTiO_3$ from Ref. 40 is included for comparison. [Reproduced with permission from J. Chem. Phys. **28**, 824 (1958). Copyright 1958 American Institute of Physics]. (b) Direct band gap analysis of these materials. The optical gap of $Ca_3Ti_2O_7$ is 3.94 eV, whereas that of the Sr-substituted and oxygen deficient systems is 3.9 and 3.7 eV, respectively.

reported in $SrTiO_3$ (and its associated layered series).[39] This trend is typical in layered perovskites including the Ruddlesden-Popper series[45,46] and is due to the fact that the octahedra, which are three-dimensionally connected in the $n = \infty$ parent compound, become systematically more isolated with decreasing *n*. At the same time, the orbitals defining the band edge in $Ca_3Ti_2O_7$ become increasingly confined, which narrows the valence band and increases the gap.[39,47] The orbital projected DOS (provided in the supplementary material)[28] and the band structure confirm this point and reveal that the bottom of the conduction band consists of in-plane, two dimensional Ti *d*-orbitals with no dispersion along the *c* axis.

Chemical substitution is a powerful technique for tuning the properties of layered perovskites.[48] This approach is motivated by the fact that stability lies in the tolerance factor, which is characterized by the relative size of the cations involved. In our work, we replaced Ca with Sr to yield $Ca_{2.5}Sr_{0.5}Ti_2O_7$. Figure 4(a) displays the optical response of $Ca_{2.5}Sr_{0.5}Ti_2O_7$; the corresponding direct gap analysis is shown in panel (b). Ca-related states are not involved in the excitations that define the leading edge of the band gap. That said, the relative size difference between Sr and Ca ions is significant, and it is the Ca ions in the perovskite layer (and not the ones in the rock salt layer) that get replaced by Sr.[7] Consequently, the octahedral rotation and tilt angle are reduced to stabilize the structure.[7,8] Since octahedral rotations in perovskites often control the electronic structure and

properties,[49–51] we anticipated that the band gap would be modulated due to Sr substitution. Our analysis instead reveals a band gap of 3.9 eV, which is only slightly lower than the 3.94 eV gap for $Ca_3Ti_2O_7$. This is in line with our DFT calculations that find when the degree of octahedral rotations is decreased, the band gap is only reduced by a minute amount.[28] We also find that the band edge is broadened slightly compared to that in pristine $Ca_3Ti_2O_7$. We therefore conclude that chemical disorder in $Ca_{2.5}Sr_{0.5}Ti_2O_7$ modifies the band gap only slightly, despite the fact that it reduces the net remnant polarization by 50% compared to the parent compound.[8]

Trends in the electronic structure that develop due to oxygen deficiencies in the Ruddlesden-Popper series are particularly interesting because the valence band is primarily comprised of O 2*p* orbitals [Fig. 3]. Oxygen vacancies are well known to introduce carriers, modify band width, and distort the local environment around the transition metal center—all of which combine to influence the electronic properties.[20,52–54] Figures 4(a) and 4(b) display the optical absorption spectrum and corresponding direct gap analysis of $Ca_3Ti_2O_{7-\delta}$. As a reminder, δ is on the order of 0.001. The band gap is 3.7 eV, markedly lower than that of pristine $Ca_3Ti_2O_7$. There is also a broad tail in the oxygen-deficient sample that persists to lower energies [Fig. 4(a)]. Similar structures are observed in oxygen deficient $CaTiO_3$ and $SrTiO_3$.[55,56] The reduced band gap and broad absorption tail in $Ca_3Ti_2O_{7-\delta}$ are primarily due to oxygen vacancies which introduce hole carriers. At the same time, oxygen deficiencies modify the local structure around the Ti centers (and therefore, the TiO_6 octahedral rotations), which according to our DFT calculations, results in a broader valence band. Clearly, control of the oxygen content is a promising strategy for band gap tuning in $Ca_3Ti_2O_7$; the technique has been used in many other ferroelectrics as well.[57] Based on these findings, we suggest that gating experiments, particularly those carried out with ionic liquids, should be carefully controlled to prevent oxygen migration.

To summarize, we combined optical spectroscopy, photoconductivity, and first principles calculations to unveil the electronic properties of $Ca_3Ti_2O_7$, a recently discovered hybrid improper ferroelectric oxide. Analysis of the linear absorption spectrum reveals a direct gap at 3.94 eV, noticeably larger than that in $CaTiO_3$ (3.4 eV) due to confinement effects in the $n = 2$ member of the Ruddlesden-Popper series. The band gap in $Ca_3Ti_2O_7$ is defined by O $p \rightarrow$ Ti d charge transfer excitations. *A*-site chemical substitution into the perovskite layer with Sr broadens the gap ever so slightly, an effect that we attribute to the influence of octahedral tilting. On the other hand, oxygen vacancies reduce the band gap to 3.7 eV and introduce a significant low energy tail. Both effects are due to the addition of hole carriers and the associated valence band broadening. An interesting extension of this work is to investigate *B* site substitution.[20] This may lead to new families of magnetoelectric multiferroics.

Research at Tennessee was supported by the U.S. Department of Energy, Office of Basic Energy Sciences, Materials Science Division under Award No. DE-FG02-01ER45885 (J.L.M.). The work performed at Rutgers was supported by the National Science Foundation under Award No. DMREF-1233349 (S.W.C. and D.V.).

[1]R. E. Cohen, Nature **358**, 136 (1992).
[2]A. von Hippel, Rev. Mod. Phys. **22**, 221 (1950).
[3]E. Bousquet, M. Dawber, N. Stucki, C. Lichtensteiger, P. Hermet, S. Gariglio, J.-M. Triscone, and P. Ghosez, Nature **452**, 732 (2008).
[4]N. A. Benedek and C. J. Fennie, Phys. Rev. Lett. **106**, 107204 (2011).
[5]A. B. Harris, Phys. Rev. B **84**, 064116 (2011).
[6]S.-W. Cheong and M. Mostovoy, Nat. Mater. **6**, 13 (2007).
[7]M. M. Elcombe, E. H. Kisi, K. D. Hawkins, T. J. White, P. Goodman, and S. Matheson, Acta Crystallogr., Sect. B: Struct. Sci. **47**, 305 (1991).
[8]Y. S. Oh, X. Luo, F.-T. Huang, Y. Wang, and S.-W. Cheong, Nat. Mater. **14**, 407 (2015).
[9]J. Y. Jo, Y. S. Kim, T. W. Noh, J.-G. Yoon, and T. K. Song, Appl. Phys. Lett. **89**, 232909 (2006).
[10]J. Wang, J. B. Neaton, H. Zheng, V. Nagarajan, S. B. Ogale, B. Liu, D. Viehland, V. Vaithyanathan, D. G. Schlom, U. V. Waghmare, N. A. Spaldin, K. M. Rabe, M. Wuttig, and R. Ramesh, Science **299**, 1719 (2003).
[11]W. Zhong and D. Vanderbilt, Phys. Rev. Lett. **74**, 2587 (1995).
[12]V. V. Lemanov, A. V. Sotnikov, E. P. Smirnova, M. Weihnacht, and R. Kunze, Solid State Commun. **110**, 611 (1999).
[13]N. A. Benedek and C. J. Fennie, J. Phys. Chem. C **117**, 13339 (2013).
[14]L. Goncalves-Ferreira, S. A. T. Redfern, E. Artacho, and E. K. H. Salje, Phys. Rev. Lett. **101**, 097602 (2008).
[15]S. Van Aert, S. Turner, R. Delville, D. Schryvers, G. Van Tendeloo, and E. K. H. Salje, Adv. Mater. **24**, 523 (2012).
[16]A. Beran, E. Libowitzky, and T. Armbruster, Can. Mineral. **34**, 803 (1996).
[17]N. A. Benedek and T. Birol, J. Mater. Chem. C **4**, 4000 (2016).
[18]T. Birol, N. A. Benedek, and C. J. Fennie, Phys. Rev. Lett. **107**, 257602 (2011).
[19]N. A. Benedek, A. T. Mulder, and C. J. Fennie, J. Solid State Chem. **195**, 11 (2012).
[20]W. L. Harrigan, S. E. Michaud, K. A. Lehuta, and K. R. Kittilstved, Chem. Mater. **28**, 430 (2016).
[21]Y. Sang, H. Liu, and A. Umar, ChemCatChem **7**, 559 (2015).
[22]H. Kato and A. Kudo, J. Phys. Chem. B **106**, 5029 (2002).
[23]J. P. Perdew, K. Burke, and M. Ernzerhof, Phys. Rev. Lett. **77**, 3865 (1996).
[24]P. E. Blöchl, Phys. Rev. B **50**, 17953 (1994).
[25]G. Kresse and D. Joubert, Phys. Rev. B **59**, 1758 (1999).
[26]G. Kresse and J. Furthmüller, Phys. Rev. B **54**, 11169 (1996).
[27]G. Kresse and J. Furthmüller, Comput. Mater. Sci. **6**, 15 (1996).
[28]See supplementary material at http://dx.doi.org/10.1063/1.4954404 for densities of state (DOS) calculations for $Ca_3Ti_2O_7$ having hypothetical structures with smaller octahedral rotation angles and polarizations. It also shows the orbital projected densities of states of Ti ions in $Ca_3Ti_2O_7$. The band structure and densities of states of $CaTiO_3$ are also shown for comparison.
[29]K. Ueda, H. Yanagi, R. Noshiro, H. Hosono, and H. Kawazoe, J. Phys.: Condens. Matter **10**, 3669 (1998).
[30]A. H. Kahn and A. J. Leyendecker, Phys. Rev. **135**, A1321 (1964).
[31]J. Tauc, Mater. Res. Bull. **3**, 37 (1968).
[32]J. I. Pankove, *Optical Processes in Semiconductors* (Dover, New York, 1971).
[33]J. Tauc, R. Grigorovici, and A. Vancu, Phys. Status Solidi B **15**, 627 (1966).
[34]E. Rey, M. R. Kamal, R. B. Miles, and B. S. H. Royce, J. Mater. Sci. **13**, 812 (1978).
[35]B. D. Viezbicke, S. Patel, B. E. Davis, and D. P. Birnie, Phys. Status Solidi B **252**, 1700 (2015).
[36]Q. C. Sun, H. Sims, D. Mazumdar, J. X. Ma, B. S. Holinsworth, K. R. O'Neal, G. Kim, W. H. Butler, A. Gupta, and J. L. Musfeldt, Phys. Rev. B **86**, 205106 (2012).
[37]B. S. Holinsworth, D. Mazumdar, H. Sims, Q.-C. Sun, M. K. Yurtisigi, S. K. Sarker, A. Gupta, W. H. Butler, and J. L. Musfeldt, Appl. Phys. Lett. **103**, 082406 (2013).
[38]M. I. Aroyo, D. Orobengoa, G. de la Flor, E. S. Tasci, J. M. Perez-Mato, and H. Wondratschek, Acta Crystallogr. Sect. A **70**, 126 (2014).
[39]C.-H. Lee, N. J. Podraza, Y. Zhu, R. F. Berger, S. Shen, M. Sestak, R. W. Collins, L. F. Kourkoutis, J. A. Mundy, H. Wang, Q. Mao, X. Xi, L. J. Brillson, J. B. Neaton, D. A. Muller, and D. G. Schlom, Appl. Phys. Lett. **102**, 122901 (2013).

[40]A. Linz and K. Herrington, J. Chem. Phys. **28**, 824 (1958).
[41]R. H. Bube, *Photoelectronic Properties of Semiconductors* (Cambridge University Press, 1992).
[42]M. Brinza, J. Willekens, M. Benkhedir, and G. Adriaenssens, in *Springer Handbook of Electronic and Photonic Materials*, edited by S. Kasap and P. Capper (Springer, USA, 2006), p. 137.
[43]G. W. Pabst, L. W. Martin, Y.-H. Chu, and R. Ramesh, Appl. Phys. Lett. **90**, 072902 (2007).
[44]F. D. Morrison, P. Zubko, D. J. Jung, J. F. Scott, P. Baxter, M. M. Saad, R. M. Bowman, and J. M. Gregg, Appl. Phys. Lett. **86**, 152903 (2005).
[45]C. Grote, B. Ehrlich, and R. F. Berger, Phys. Rev. B **90**, 205202 (2014).
[46]Z.-T. Zhu, J. L. Musfeldt, H.-J. Koo, M.-H. Whangbo, Z. S. Teweldemedhin, and M. Greenblatt, Chem. Mater. **14**, 2607 (2002).
[47]S. E. Reyes-Lillo, T. Rangel, F. Bruneval, and J. B. Neaton, e-print arXiv:1605.01818.
[48]T. Wolfram and S. Ellialtioglu, *Electronic and Optical Properties of d-Band Perovskites* (Cambridge University Press, Cambridge, 2006).
[49]A. T. Mulder, N. A. Benedek, J. M. Rondinelli, and C. J. Fennie, Adv. Funct. Mater. **23**, 4810 (2013).
[50]M. J. Pitcher, P. Mandal, M. S. Dyer, J. Alaria, P. Borisov, H. Niu, J. B. Claridge, and M. J. Rosseinsky, Science **347**, 420 (2015).
[51]F. Li, C. Song, Y. Y. Wang, B. Cui, H. J. Mao, J. J. Peng, S. N. Li, G. Y. Wang, and F. Pan, Sci. Rep. **5**, 16187 (2015).
[52]W. Lu, P. Yang, W. D. Song, G. M. Chow, and J. S. Chen, Phys. Rev. B **88**, 214115 (2013).
[53]H. Liu, F. Zeng, Y. Lin, G. Wang, and F. Pan, Appl. Phys. Lett. **102**, 181908 (2013).
[54]C. Mitra, C. Lin, J. Robertson, and A. A. Demkov, Phys. Rev. B **86**, 155105 (2012).
[55]J. Milanez, A. T. d. Figueiredo, S. d. Lazaro, V. M. Longo, R. Erlo, V. R. Mastelaro, R. W. A. Franco, E. Longo, and J. A. Varela, J. Appl. Phys. **106**, 043526 (2009).
[56]E. Orhan, F. M. Pontes, M. A. Santos, E. R. Leite, A. Beltrán, J. Andrés, T. M. Boschi, P. S. Pizani, J. A. Varela, C. A. Taft, and E. Longo, J. Phys. Chem. B **108**, 9221 (2004).
[57]S. R. Basu, L. W. Martin, Y. H. Chu, M. Gajek, R. Ramesh, R. C. Rai, X. Xu, and J. L. Musfeldt, Appl. Phys. Lett. **92**, 091905 (2008).